



Contents lists available at ScienceDirect

Cancer Letters

journal homepage: [www.elsevier.com/locate/canlet](http://www.elsevier.com/locate/canlet)

## Rottlerin induces autophagy and apoptosis in prostate cancer stem cells via PI3K/Akt/mTOR signaling pathway

Dhruv Kumar<sup>a</sup>, Sharmila Shankar<sup>b</sup>, Rakesh K. Srivastava<sup>a,\*</sup>

<sup>a</sup> Department of Pharmacology, Toxicology and Therapeutics, and Medicine, The University of Kansas Medical Center, 3901 Rainbow Boulevard, Kansas City, 66160, USA

<sup>b</sup> Department of Pathology and Laboratory Medicine, The University of Kansas Medical Center, 3901 Rainbow Boulevard, Kansas City, KS 66160, USA

### ARTICLE INFO

#### Article history:

Received 27 August 2013

Received in revised form 1 October 2013

Accepted 1 October 2013

Available online xxxxx

#### Keywords:

Autophagy

AMPK

mTOR

PI3K

Akt

LC3

### ABSTRACT

Autophagy plays an important role in cellular homeostasis through the disposal and recycling of cellular components. Cancer stem cells (CSCs) play major roles in cancer initiation, progression, and drug resistance. Rottlerin (Rott) is an active molecule isolated from *Mallotus philippinensis*, a medicinal plant used in Ayurvedic Medicine for anti-allergic and anti-helminthic treatments, demonstrates anticancer activities. However, the molecular mechanisms by which it induces autophagy in prostate CSCs have not been examined. The main objective of the paper was to examine the molecular mechanisms by which Rott induces autophagy in prostate CSCs. Autophagy was measured by the lipid modification of light chain-3 (LC3) and the formation of autophagosomes. Apoptosis was measured by flow cytometer analysis. The Western blot analysis was used to examine the effects of Rott on the expression of PI3K, phosphorylation of Akt, phosphorylation of mTOR, and phosphorylation of AMPK in pros CSCs. RNAi technology was used to inhibit the expression of Beclin-1 and ATG-7. Rott induced the lipid modification of light chain-3 (LC3) and the formation of autophagosomes after 24 h of Rott treatment in prostate CSCs. Rott-treated prostate CSCs induced transition from LC3-I to LC3-II, a hall mark of autophagy. Rott also induced the expression of Atg5, Atg7, Atg12 and Beclin-1 proteins during autophagy. The knock-down of Atg7 and Beclin-1 blocked Rott-induced autophagy. Furthermore, Rott induced AMPK phosphorylation was blocked by 3-MA, Baf and CHX. In addition, inhibition of AMPK expression by shRNA blocked Rott induced autophagy. In conclusion, a better understanding of the biology of autophagy and the pharmacology of autophagy modulators has the potential for facilitating the development of autophagy-based therapeutic interventions for prostate cancer.

© 2013 Elsevier Ireland Ltd. All rights reserved.

### 1. Introduction

Autophagy plays an important role in the conservation of cellular energy and for cell survival in stress condition [1,2]. It is also involved in cellular development [3], several catabolic processes, autoimmunity [4], degradation of intracellular organelles and long-lived proteins, and cell death [5,6]. Autophagy is up-regulated when cells faces environmental stressors such as pathogen infection, nutrient starvation and chemotherapeutic agents [7–10], and the process is essential for the maintenance of cellular energy,

and thereby, for cell survival in stress conditions [1,2]. Although autophagy is initiated as a protective response to stress, the constitutive activation of autophagy can lead to cell death by unnecessary self-degradation of important cellular components [11].

Activation of AMPK are among the major regulators of autophagy [12], which are involved in biosynthesis, protein folding and modification of various soluble and insoluble proteins [13]. Activation of AMPK also activates autophagy by upregulating Atg12 and LC3 conversion [14]. Recently several Atg genes [15] which have been implicated in drug-induced autophagosome formation [16] have been described [17,18]. For example, Atg6, Atg12 and Atg8 (LC3 in mammals) involves in the nucleation and elongation of autophagosomes [17]. Atg7 is essential to recruit other proteins to the autophagosomal membrane and to form autophagic vacuole in autophagy pathway [18,19]. All together, they form autophagic membrane, this membrane assembles around damaged organelles, proteins, and cytoplasm. Later, the outer membrane of autophagosomes is fused by endosomes or lysosomes to form autolysosomes

*Abbreviations:* AMPK, 5' adenosine monophosphate-activated protein kinase; Atg, autophagy related gene; Baf, bafilomycin; CHX, cycloheximide; CSCs, cancer stem cells; DAPI, 4',6-diamidino-2-phenylindole; FBS, fetal bovine serum; LC3, microtubule-associated protein 1 light chain 3; mTOR, mammalian target of rapamycin; PI3K, phosphatidylinositol 3-kinases; Rott, rottlerin.

\* Corresponding author. Tel.: +1 913 945 6686.

*E-mail addresses:* [dkumar2@kumc.edu](mailto:dkumar2@kumc.edu) (D. Kumar), [sshankar@kumc.edu](mailto:sshankar@kumc.edu) (S. Shankar), [rsrivastava@kumc.edu](mailto:rsrivastava@kumc.edu) (R.K. Srivastava).

0304-3835/\$ - see front matter © 2013 Elsevier Ireland Ltd. All rights reserved.

<http://dx.doi.org/10.1016/j.canlet.2013.10.003>

Please cite this article in press as: D. Kumar et al., Rottlerin induces autophagy and apoptosis in prostate cancer stem cells via PI3K/Akt/mTOR signaling pathway, *Cancer Lett.* (2013), <http://dx.doi.org/10.1016/j.canlet.2013.10.003>

where lysosomal hydrolases degrade the cytoplasm derived contents of autophagosome together with its inner membrane and presented to citric acid cycle for energy generation [20]. Furthermore, an important autophagy-regulatory gene Beclin-1 functions as a haploinsufficient tumor suppressor gene [21] which can regulate autophagic cell death and apoptosis.

In spite of these advances, the relationship between autophagy and apoptosis in CSCs is still not well understood. CSCs may be responsible for self-renewal/maintenance, tumor onset and metastasis and mutation accumulation [22]. In CSCs, autophagy plays an important role in the regulation of drug resistance, self-renewal, tumorigenic potential [18,19,23–26,34] and cell differentiation, suggesting autophagy could be a promising therapeutic target in a subset of cancers. In some studies, both autophagy and apoptosis have been reported in the same cells [25–28], and they may be interrelated by some signaling pathway [11,15,21,29,31]. The PI3K/Akt/mTOR and AMPK signaling pathway is a key regulator of autophagy and apoptosis. Several anti-apoptotic signals such as the PI3K/Akt/mTOR signaling pathway and Bcl-2 suppress autophagy [15,29] and concurring-apoptotic signals such as the AMPK signaling pathway and Bax activate autophagy [30].

Rott, a plant derived chemotherapeutic agent has been used as a protein kinase C-delta signaling pathway inhibitor [31]. It inhibits cell propagation and induces apoptosis through mitochondrial membrane depolarization. In several human cancer cells, Rott has been shown to induce a starvation response, which is a key regulator of autophagy [32,33]. Since prostate cancer contains rare CSCs, we sought to examine the molecular mechanism by which Rott induces autophagy in prostate CSCs. Here we report that Rott induced early autophagy is mainly dependent on the induction of autophagosomes, conversion of LC3-I – LC3-II, expression of Atg12 and Beclin-1 and inhibition of Bcl-2, Bcl-xL, XIAP and cIAP-1. Eventually, Rott induced apoptosis through the inhibition of PI3K/Akt/mTOR and AMPK pathways, and activation of caspases. Moreover, inhibition of AMPK by shRNA blocked Rott-induced autophagy, suggesting AMPK plays a crucial role in Rott-induced apoptosis. These findings strongly suggest that Rott-induced autophagy may also play some role to induce apoptosis in prostate CSCs.

## 2. Materials and methods

### 2.1. Cell culture and reagents

Rott, 3-MA, CHX, Baf, and puromycin were obtained from Sigma-Aldrich Corp. (St. Louis, MO). Anti-human LC3 (3868S), Atg5 (8540S), Atg7 (8558S), Atg12 (4180S), Beclin-1 (3495S), Bax (5023S), Bcl-2 (2876S), Bcl-XL (2764S), cIAP-1 (7065S), Akt (9272S), pAkt (2965S), mTOR (2983S), pmTOR (2976S) and XIAP (2045S), AMPK (5831S), pAMPK (2537S) and  $\beta$ -actin (4970S) antibodies were accepted from Cell Signaling Technology (Danvers, MA). Atg7, Beclin-1 and AMPK shRNA were obtained from Open Biosystems (Lafayette, CO).

Human prostate tumor samples were minced and enzymatically dissociated with 1 mg/ml collagenase D (Roche, Indianapolis, IN) and 1  $\mu$ g/ml DNase I (Roche) for 1 h at 37 °C, and then sequentially filtered through 100 and 70  $\mu$ m cell strainers (BD, Franklin Lakes, NJ). After the lysis of red blood cells with Red Blood Cell Lysis Solution (Miltenyi Biotec Inc., Auburn, CA), the filtered cells were grown in Stem Cell Growth Medium (Celprogen, San Pedro, CA) supplemented with 1% N2 (Life Technologies, Carlsbad, CA), 2% B27 (Life Technologies), 20 ng/ml human basic fibroblast growth factor (bFGF) (Life Technologies), 100 ng/ml epidermal growth factor (Life Technologies) and 1% antibiotic-antimycotic (Life Technologies) on ultralath attachment culture dishes (Corning Inc., Corning, NY, USA) at 37 °C in a humidified atmosphere of 95% air and 5% CO<sub>2</sub>. Dissociated single cells were filtered and double-stained with a phycoerythrin (PE)-conjugated monoclonal antibody against CD44 (G44-26; BD Biosciences, San Jose, CA) and an allophycocyanin (APC)-conjugated monoclonal antibody against CD133 (AC133; Miltenyi Biotec). Isotype-matched mouse immunoglobulins were used as controls. Stained cells were sorted using the FACS Aria II Cell Sorter (BD Bioscience).

### 2.2. XTT assay

Prostate CSCs (1  $\times$  10<sup>4</sup> in 200  $\mu$ l culture medium per well) were seeded in 96-well plate (flat bottom), treated with Rott (0, 0.5, 1 and 2  $\mu$ M), and incubated for 48 h at 37 °C and 5% CO<sub>2</sub>. Before the end of the experiment, 50 ml XTT labeling

mixture (final concentration, 125  $\mu$ M XTT (sodium 2,3-Bis(2-methoxy-4-nitro-5-sulfophenyl)-2H-tetrazolium-5-carboxanilide inner salt) and 25  $\mu$ M PMS (phenazine methosulphate) per well was added and plates were incubated for further 4 h at 37 °C and 5% CO<sub>2</sub>. The spectrophotometric absorbance of the sample was measured using a microtiter plate (ELISA) reader. The wavelength to measure absorbance of the formazan product was 450 nm, and the reference wavelength was 650 nm.

### 2.3. Vacuolated cell accounting

Cells were seeded in 6-well plates at a density of 10  $\times$  10<sup>4</sup> cells/well in complete medium and incubated overnight. Cells were then treated with various concentration of Rott (0, 0.5, 1, and 2  $\mu$ M) for 48 h. Vacuolated cells were counted using fluorescent microscope in at least 100 cells for each condition.

### 2.4. pEGFP-LC3 transfection

pEGFP-LC3 plasmid were transfected in prostate CSCs by using neon electroporator at 1400 V, 2-pulses for 20 ms. 1  $\times$  10<sup>6</sup> cells were seeded in medium sized tissue culture flask 2 days prior to transfection. After 48 h of cell growth cells were harvested by trypsinizing with 25%EDTA. Cells were centrifuged to get cell pellet. Cells were resuspended in 100  $\mu$ l R-buffer obtained from Invitrogen. 30  $\mu$ g of DNA were mixed with the suspended cells and electroporated by using 100  $\mu$ l neon tips. After electroporation, pEGFP-LC3 transfected prostate CSCs cells were seeded in 60 mm culture dish. After 2 days of electroporation transfected cells were selected by using 10  $\mu$ M neomycin, and visualized under Leica 6000B microscope with 10X objectives.

### 2.5. Lentiviral particle production and AMPK, Atg7 and Beclin-1 transduction

AMPK shRNA, Atg7 shRNA and Beclin-1 shRNA were obtained from Open Biosystems (Lafayette, CO). Lentivirus particles were produced by triple transfection of HEK 293T cells. Packaging 293T cells were plated in 10-cm plates at a cell density of 5  $\times$  10<sup>6</sup>. Transfection of packaging cells and infection of prostate CSCs were carried out using standard protocols with some modifications. In brief, 293T cells were transfected with 8 mg of plasmid and 4 mg of lentiviral vector using lipid transfection (Lipofectamine-2000) according to the manufacturer's protocol. Viral supernatants were collected and concentrated by adding PEG-it virus precipitation solution (SBI System Biosciences, Mountain View, CA). Prostate CSCs were transduced with viral particles expressing scrambled, AMPK shRNA, Atg7 shRNA or Beclin-1 shRNA.

### 2.6. Immunofluorescence assay

Cells were grown on fibronectin-coated coverslips (Beckton Dickinson, Bedford, MA), and treated with Rott (0, 0.5, 1 and 2  $\mu$ M), washed in PBS, and fixed for 15 min in 4% paraformaldehyde. Cells were permeabilized in 0.1% Triton X-100, washed, and blocked in 10% normal goat serum. After blocking, cells were incubated with primary antibody (1:100) for 18 h at 4 °C, washed with PBS and incubated with fluorescently labeled secondary antibody (1:200) along with 4, 6-diamido-2-phenylindole hydrochloride (DAPI) (1 mg/ml) for 1 h at room temperature. Finally, coverslips were washed and mounted using vectashield (Vector Laboratories, Burlington, CA). Isotype-specific negative controls were included with each staining. Stained cells were mounted and visualized under Leica 6000B microscope with 100 $\times$  objectives. The number of cells expressing punctate and the number of punctate per cell were counted manually.

### 2.7. Nuclear staining with DAPI

After Rott treatment, adherent cells were fixed for 20 min at room temperature with 4% paraformaldehyde and permeabilized for 10 min with 0.2% Triton X-100 in PBS. After PBS washes, cells were stained with 4, 6-diamido-2-phenylindole hydrochloride (DAPI) in PBS at the concentration of 1 mg/ml for 15 min at room temperature. Cells were then washed with PBS and visualized using Leica 6000B microscope with 100 $\times$  objectives.

### 2.8. Electron microscopy assay

To demonstrate the induction of autophagy in Rott-treated prostate CSCs, cells were treated with (0, 0.5, 1, and 2  $\mu$ M) of Rott for 24 h, cells were harvested by trypsinization, washed and fixed in 2.0% glutaraldehyde in 0.1 M phosphate buffer, then post-fixed in 1% osmium tetroxide buffer. After dehydration in a graded series of ethanol, the cells were embedded in spur resin. Thin sections (60 nm) were cut on an Ultramicrotome. The sectioned grids were stained with saturated solutions of uranyl acetate and lead citrate. The sections were examined by electron microscope.

### 2.9. Whole-cell lysates preparation

After treatment with Rott (0, 0.5, 1 and 2  $\mu$ M), prostate CSCs were pelleted by centrifugation at 1000  $\times$  rpm for 5 min and washed once with PBS. Cells were then resuspended in RIPA buffer (50 mM Tris-HCl, pH 7.5, 150 mM NaCl, 1% v/v Nonidet P-40, 0.5% v/v sodium deoxycholate and 0.1% SDS) supplemented with protease inhibitor cocktail (Sigma) and phosphatase inhibitor cocktail (Sigma), and lysed on ice by sonicating for 5 s and 5–10 pulses. The lysates were centrifuged for 20 min at 12000 $\times$ g and supernatant was collected and used for further experiments.

### 2.10. Western blotting

Total cellular lysates were obtained by lysing cells in a buffer containing RIPA buffer (50 mM Tris-HCl, pH 7.5, 150 mM NaCl, 1% v/v Nonidet P-40, 0.5% v/v sodium deoxycholate and 0.1% SDS), and a mixture of protease and phosphatase inhibitors. Lysates were sonicated for 5 s and 5–10 pulses, centrifuged for 20 min at 12000 $\times$ g and stored at  $-80^{\circ}\text{C}$ . Equal amounts of lysate proteins (50–60  $\mu$ g total protein) were electrophoretically separated by 10% sodium dodecyl sulfate-polyacrylamide gel electrophoresis (SDS-PAGE) and transferred to nitrocellulose membrane. Nitrocellulose blots were blocked with 5% nonfat dry milk in TBS-T (TBS and 0.01% Tween-20) buffer (20 mM Tris-HCl (pH 7.4), and 500 mM NaCl), and incubated with primary antibody in TBS-T overnight at  $4^{\circ}\text{C}$ . Immunoblots were washed three times (5, 5, and 5 min each) with TBS-T followed by 2–3 h incubation in secondary antibody. Chemiluminescence reactions were carried out according to the Super Signal West Pico substrate (Thermo Fisher, Waltham, MA) protocol. Antibody dilutions were carried out as per the data sheet provided by the manufacturer or

as suggested by the provider's laboratory. Blots were stripped for reuse by washing for 30 min to 2 h in TBS-T buffer (pH 2.0–2.5) at room temperature. Blots were visualized using SuperSignal West Pico substrate (Thermo Fisher, Waltham, MA) and conversion of LC3-I (18 kDa) to LC3-II (16 kDa) were detected by X-ray film analyzer.

### 2.11. Apoptosis analysis by flow cytometer

Prostate CSCs (10,000 cells/well) were seeded in 6 well plate and exposed to Rott (0, 0.5, 1 and 2  $\mu$ M). Cells were then washed in PBS and collected by trypsinization, and fixed overnight in 70% glacial ethanol. Next day cells were washed in PBS and resuspended in 1 mL of PBS containing 50  $\mu$ g/mL RNase and incubated at  $37^{\circ}\text{C}$  for 2 h. 50  $\mu$ g/mL propidium iodide (PI) added in resuspended cells and then incubated for 60 min in dark at  $4^{\circ}\text{C}$ . Cell cycle analysis was performed by flow cytometry (Becton Dickinson, Franklin Lakes, NJ, USA), and the population of cells in each phase was calculated using the Cell Quest software program. Each experiment was conducted three times.

Prostate CSCs (10,000 cells/well) were seeded in 6 well plate and exposed to Rott (0, 0.5, 1 and 2  $\mu$ M). Treated cells were washed twice with cold PBS and resuspended in buffer at a concentration of  $10^6$  per ml. Cells were mixed with 10  $\mu$ l of fluorescence isothiocyanate (FITC)-conjugated annexin-V reagent and 10  $\mu$ l of 3 mM propidium iodide (PI). After 15 min incubation at room temperature in the dark and further washings, samples were analyzed by flow cytometry. Flow cytometry was performed with a FACScan analyzer (Becton Dickinson, Franklin Lakes, NJ, USA) with 15 mW argon ion laser (488 nm) and Cell Quest software. Annexin-V staining was detected in the FL1 channel, whereas PI staining was monitored in the FL2 channel: appropriate quadrants were set and the percentage of cells negative for stains (viable cells), positive for annexin-V (apoptotic cells) and positive for PI (dead cells) were acquired.

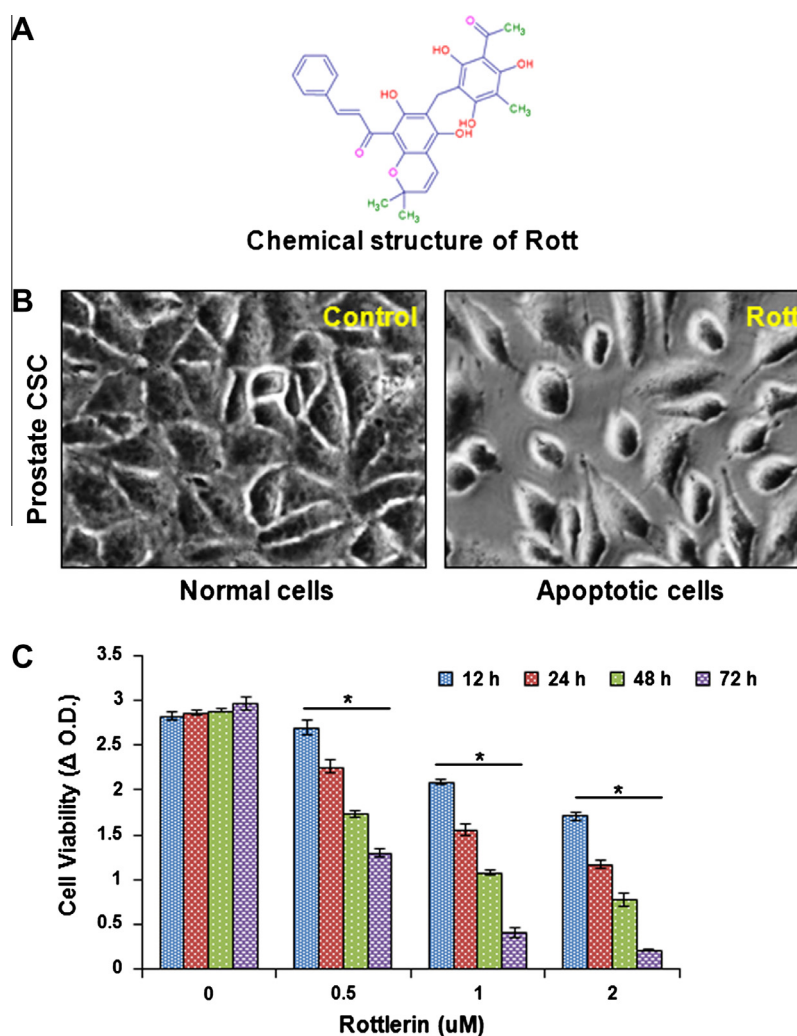


**Fig. 1.** Rott inhibited cell viability, and induced apoptosis in prostate CSCs. A. Structural representation of plant derived chemopreventive agent Rott. B. Prostate CSCs were treated with Rott (0, 2  $\mu$ M) for 48 h, and the apoptosis was monitored under phase contrast microscope. C. Cells were grown in complete medium and treated with Rott (0, 0.5, 1 and 2  $\mu$ M) for different time points. Cell viability was measured by XTT assay. Blue color (12 h), red (24 h), green (48 h), and violet (72 h). (For interpretation of the references to colour in this figure legend, the reader is referred to the web version of this article.)

### 3. Results

#### 3.1. Rott induced cell death and inhibited cell viability in prostate CSCs

To examine whether Rott induces apoptosis in prostate CSCs, we exposed prostate CSCs with Rott (2  $\mu$ M) for 48 h and showed cell death under phase contrast microscope (Fig. 1B). To investigate the cytotoxic effect of Rott on prostate CSCs, we treated prostate CSCs with different concentrations of Rott (0, 0.5, 1, and 2  $\mu$ M) for various time points (12, 24, 48, and 72 h). Rott inhibited cell viability in a time- and dose-dependent manner (Fig. 1C). While the treatment with 0.5  $\mu$ M Rott had little effect, treatments with 1 or 2  $\mu$ M Rott for 48 and 72 h significantly inhibited cell viability.

#### 3.2. Rott induced cytoplasmic vacuolation in prostate CSCs

To examine the cytotoxic effect and cytoplasmic vacuolation on prostate CSCs, we treated prostate CSCs with different concentrations of Rott (0, 0.5, 1 and 2  $\mu$ M) for 24 h. Rott induced cytotoxicity in prostate CSCs by forming cytoplasmic vacuolation

in a dose-dependent manner (Fig. 2A). Rott with concentration 1  $\mu$ M and 2  $\mu$ M induced more cytoplasmic vacuolation in prostate CSCs compared to 0.5  $\mu$ M (Fig. 2A and C). Co-treated prostate CSCs with Rott (2  $\mu$ M) and Baf (10 nM), 3-MA (10 mM) or CHX (35  $\mu$ M) inhibited cytoplasmic vacuolation (Fig. 2B and D). Moreover, the prostate CSCs treated with Rott showed morphological features of cytoplasmic vacuole accumulation. Rott increased more numbers of vacuole formation in the cytoplasm of prostate CSCs.

#### 3.3. Rott induced autophagy in prostate CSCs

LC3 is a hallmark of autophagy and the conversion of LC3-I – LC3-II via proteolytic cleavage and lipidation shows autophagy induction. Therefore, to study whether Rott induced autophagy in prostate CSCs, the formation of LC3 dots and conversion of LC3-I – LC3-II were examined by different molecular technique. This modification of LC3 is essential for the formation of autophagosomes and for the completion of macroautophagy. To confirm whether LC3 (autophagosomes) is redistributed after Rott treatment, we observed the prostate CSCs after transfection of

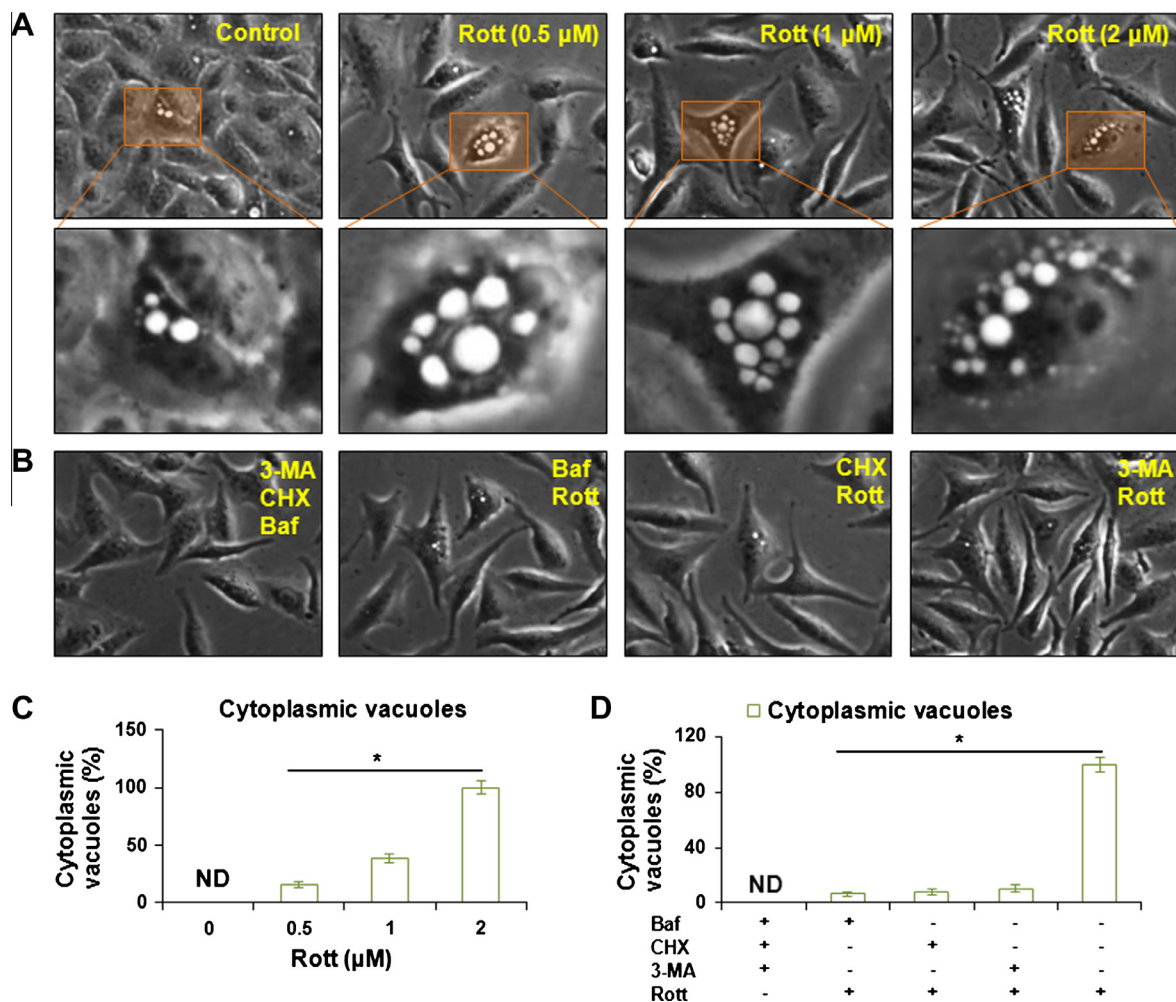


**Fig. 2.** Rott induced apoptosis and cytoplasmic vacuolation in prostate CSCs. A. Cells were grown in complete medium and treated with Rott (0, 0.5, 1, and 2  $\mu$ M) for 24 h. Representative images were obtained by phase contrast microscopy. Magnification, 20 $\times$ . Inserts show the cytoplasmic vacuoles developed by the effect of different concentration of Rott (0, 0.5, 1 and 2  $\mu$ M), and the autophagic vacuoles were counted under phase contrast microscope. B. Prostate CSCs were co-treated with Rott (2  $\mu$ M) and Baf (10 nM), 3-MA (10 mM) or CHX (35  $\mu$ M) for 24 h, and the autophagic vacuoles were counted under phase contrast microscope. C. Kinetic measurement of autophagic vacuoles in prostate CSCs treated with Rott (0, 0.5, 1 and 2  $\mu$ M) for 24 h. D. Kinetic measurement of autophagic vacuoles in prostate CSCs co-treated with Rott (2  $\mu$ M) and Baf (10 nM), 3-MA (10 mM) or CHX (35  $\mu$ M) for 24 h. Data are reported as the mean  $\pm$  standard error (SE) of percentage of cells.  $n = 5$ ,  $P < 0.05$  when compared with Rott treated in an identical manner.

PEGFP-LC3 (Fig. 3A). Cells were cultured in complete medium, treated with or without Rott and subjected to immunofluorescence for visualization of pEGFP-LC3 transfected cells. Our results indicated that Rott induced autophagy in a dose dependent manner (Fig. 3A). We next counted and graded CSCs based on abundance of LC3 positive staining. The number of LC3 positive CSCs and severity of autophagic response per cell (number of autophagosomes present per cell) was increased following Rott treatment at 48 h (Fig. 3B). To examine whether cells vacuolation induced by Rott is related to autophagy, prostate CSCs were treated with Rott (0, 0.5, 1, and 2  $\mu$ M) for 24 h and the ultrastructure of cells were analyzed by electron microscopy (Fig. 3C). Numerous autophagic vacuoles containing lamellar structures or residual digested material and empty vacuoles were observed in the prostate CSCs when treated with 1 and 2  $\mu$ M of Rott, indicating that Rott not only increased the number of vacuoles, but also increased the number of mature autophagosomes formed per cell (Fig. 3C). However, the co-treated prostate CSCs with Rott (2  $\mu$ M) and Baf (10 nM), 3-MA (10 mM) or CHX (35  $\mu$ M) inhibited autophagy (Fig. 3D). 3-MA is a PI3K inhibitor which is essential for the autophagic process and the autophagy inducing potential of Rott was partially reverted with 3-MA, indicating that inhibition of PI3K reduced the number of cells undergoing autophagy. Baf is a potent and specific inhibitor of vacuolar (H<sup>+</sup>)-ATPase (V-ATPase) which stops the acidification of lysosomes during the formation of autophagosomes and slows

down the lipidation of LC3 protein. CHX, a small molecule inhibitor of protein synthesis, blocks the elongation phase of eukaryotic translation [35].

#### 3.4. Molecular signals of regulation of autophagy in prostate CSCs

To determine whether Rott regulates autophagy at 24 h, first we examined the levels of LC3-II, which is an LC3-phosphatidylethanolamine conjugate and a promising autophagosomal marker. Rott induced an increase in the lipidated form of LC3 (LC3-II) at 24 h in concentration dependent manner (Fig. 4A). We next measured the expression of autophagy-related proteins, Atg5, Atg7, Atg12 and Beclin-1 in prostate CSCs treated with Rott (Fig. 4A). The levels of Atg5, Atg7, Atg12 and Beclin-1 expression were increased in a dose dependent manner following treatment with Rott. These results indicate that Rott stimulated not only the conversion of a fraction of LC3-I into LC3-II but also caused the accumulation of Atg5, Atg7, Atg12 and Beclin-1 proteins. The cellular levels of Bcl-2, Bcl-xL, XIAP and cIAP-1 proteins were significantly decreased after the treatments with Rott for 48 h (Fig. 4B). The accumulation of Atg5, Atg7, Atg12 and Beclin-1 proteins may be mediated by the reduction in Bcl-2 and Bcl-xL expression. To assess how the pro-apoptotic effect of Rott was linked to the autophagy signal, we used Baf, 3-MA or CHX. Treatment of prostate CSCs with Baf, 3-MA or CHX inhibited Rott induced conversion of LC-3, and induction of Atg5,

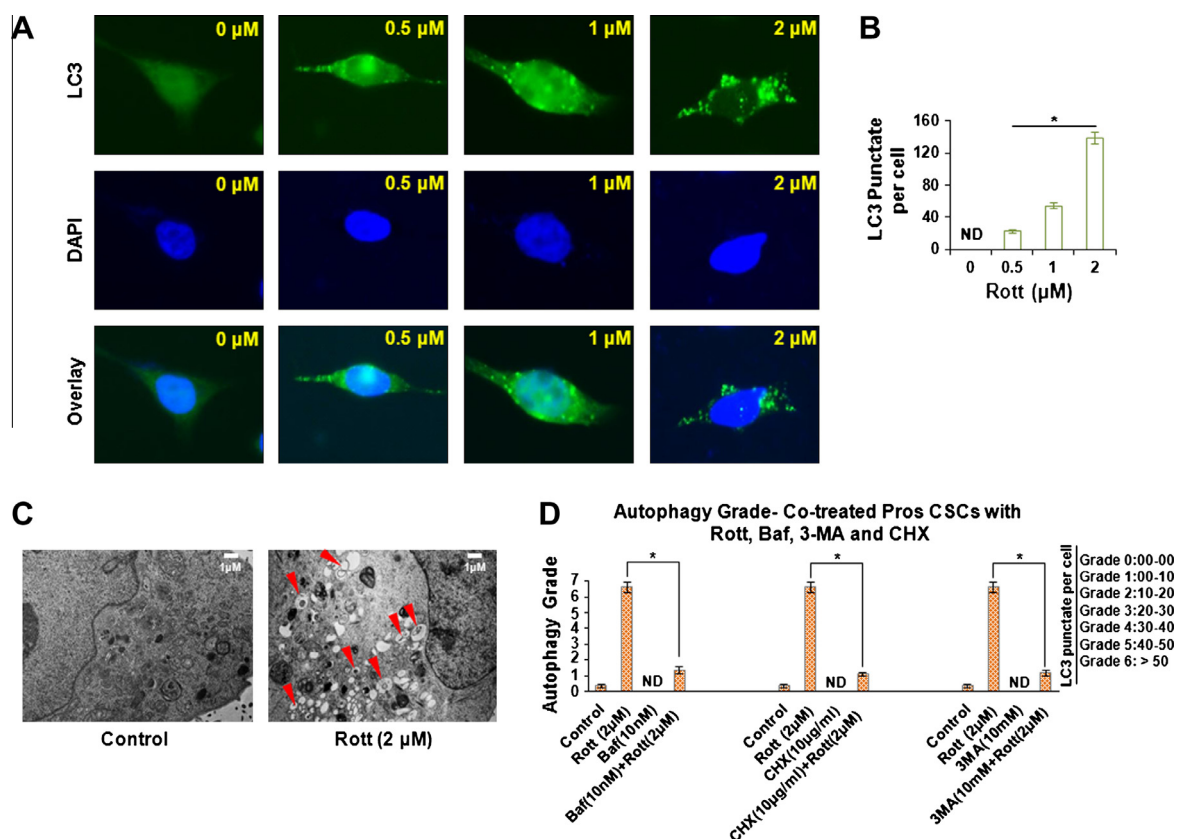


**Fig. 3.** Rott induced autophagy in prostate CSCs. A. Redistribution of pEGFP-LC3. Prostate CSCs were stably transfected with a pEGFP-LC3 fusion construct and cultured in complete media, and treated with Rott (0, 0.5, 1, and 2  $\mu$ M) for 24 h. Cells were visualized under a fluorescence microscope to examine the expression of LC3-II. LC3 expression increases by increasing Rott concentration in prostate CSCs. B. Punctate dot quantification in pEGFP-LC3-positive prostate CSCs treated with Rott (0, 0.5, 1 and 2  $\mu$ M) for 24 h. Quantitation of punctate dot per cell based on number of punctate dot in pEGFP-LC3-positive cells. Quantitation represents at least 100 cells counted and scored per treatment. C. Electron microscopy shows the ultrastructure of prostate CSCs treated with different concentrations of Rott (0 and 2  $\mu$ M) in complete medium for 24 h. Arrows indicate autophagosomes including residual digested material (red arrow). D. Punctate dot quantification in pEGFP-LC3-positive prostate CSCs co-treated with Rott (2  $\mu$ M) and Baf (10 nM), 3-MA (10 mM) or CHX (35  $\mu$ M) for 24–48 h. Quantitation of punctate dot per cell based on number of punctate dot in pEGFP-LC3-positive cells. Quantitation represents at least 100 cells counted and scored per treatment. Rott induces autophagy in prostate CSCs. Data are reported as the mean  $\pm$  standard error (SE) of percentage of cells.  $n = 5$ ,  $^*P < 0.05$  when compared with Rott (2  $\mu$ M) treated in an identical manner. (For interpretation of the references to colour in this figure legend, the reader is referred to the web version of this article.)

Atg7, Atg12 and Beclin-1 (Figs. 6E and F and 7F), suggesting that Rott has potential to induce autophagy in CSCs. Rott increased expression of Beclin-1 in a dose dependent manner in prostate CSCs.

### 3.5. Rott induced autophagy is regulated via activation of AMPK pathway

Several recent studies have shown that activation of AMPK is important in regulating autophagy. We examined whether this was the case in our model. The Western blot data showed that Rott activated AMPK by phosphorylating at Thr-172 in prostate CSCs (Fig. 4B). Further, to confirm the role of AMPK in Rott induced autophagy, we exposed the cells to Baf, 3-MA or CHX before treating with Rott. Our results as demonstrated in (Figs. 6E and F, and 7F) that are treating prostate CSCs with Baf, 3-MA or CHX inhibited Rott induced activation of AMPK. Interestingly, blocking AMPK activation also blocked the expression of LC3, Atg7 and Beclin-1 in prostate CSCs, this indicating that AMPK also mediates the effect of Rott on autophagy. These results strongly establish that AMPK is a major regulator of Rott induced autophagy in prostate CSCs.

AMPK is an energy sensor that plays a key role in the regulation of protein and lipid metabolism in response to changes in fuel availability. When activated, AMPK promotes energy-producing catabolic pathways including autophagy while inhibiting anabolic pathways. To investigate the mechanism of Rott-induced autophagy in prostate CSCs, we inhibited autophagy by AMPK shRNA. As shown in (Fig. 4D), overexpression of AMPK shRNA suppressed Rott-induced autophagy, suggesting the requirement of AMPK in Rott-induced autophagy.

### 3.6. Rott induced apoptosis via inhibition of PI3K/Akt/mTOR pathway

PI3K/Akt/mTOR signaling pathway is well-known survival pathway involved in the regulation of cell cycle, cellular transformation, cell growth, and tumorigenesis. To investigate the upstream inhibition of PI3K, mTOR by Rott, we examined Ser473 phosphorylation of Akt. As shown in (Fig. 4C), treatment with Rott decreased the levels of phosphorylated Akt and mTOR in prostate CSCs. These data suggest that Rott induces apoptosis by inhibiting PI3K/Akt/mTOR pathway. To gain further insight into the mechanism by which Rott induces cell death, we examined the effects of Rott on the expression of apoptosis-related proteins (Fig. 4B and C). Treatment of prostate CSCs with Rott resulted in cleavage of caspase-3 and caspase-9. Furthermore, the levels of IAP family proteins, such as XIAP and cIAP-1, which bind to caspases and lead to their inactivation were down regulated by Rott treatment. Moreover, the cellular levels of anti-apoptotic Bcl-2 and Bcl-xL proteins were significantly decreased, whereas pro-apoptotic Bax level was increased in response to Rott, indicating Rott induced cell death in CSCs due to an increase in the relative ratio of Bax/Bcl-2 (and/or Bcl-xL) expression.

### 3.7. Rott induced apoptosis in prostate CSCs

We studied the Rott-induced autophagy in prostate CSCs followed by apoptosis by using flow cytometer. Rott did not significantly induce apoptosis in prostate CSCs at 24 h, but significantly induced apoptosis at 48–72 h (Fig. 5A and E). Prostate CSCs treated with different concentration of Rott (0, 0.5, 1 and 2  $\mu$ M) underwent apoptosis as assessed by flow cytometer using propidium iodide (PI) and annexin-V/propidium iodide through flow cytometry (Fig. 5A–E). Cells underwent apoptosis quickly showed an increase in annexin-V binding by increasing Rott concentration but excluded propidium iodide (early apoptosis). At later time-points, the percentage of propidium iodide-staining prostate CSCs

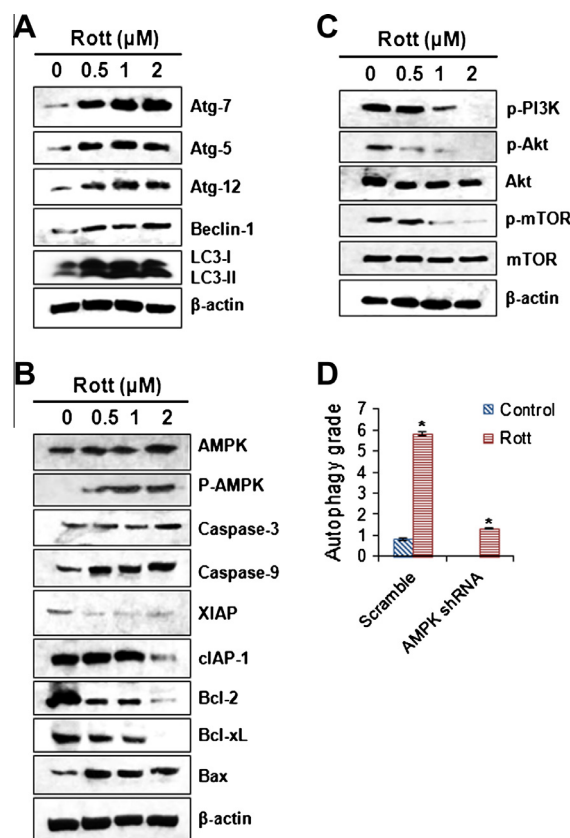


**Fig. 4.** Western blot analysis of Rott treated prostate CSCs. Prostate CSCs were grown in complete medium and treated with Rott (0, 0.5, 1, and 2  $\mu$ M) for 24–48 h, the cells were lysed and cellular proteins were then separated in SDS–polyacrylamide gels, after which they were transferred onto nitrocellulose membranes. A. The membrane was then probed with anti-LC3 antibody or  $\beta$ -actin antibody. Rott regulates autophagy-related genes in prostate CSCs. Representative blots show the concentration dependent effect of Rott on prostate CSCs. Rott regulates autophagy-related genes in prostate CSCs. The Western blot analysis was performed to measure the expression of LC3, Atg7, Atg5, Atg12, Beclin-1, and  $\beta$ -actin. B. Prostate CSCs were grown in complete medium and treated with Rott (0, 0.5, 1 and 2  $\mu$ M) for 48 h. The Western blot analysis was performed to measure the expression of active caspase-3, active caspase-9, AMPK, p-AMPK, Bax, XIAP, cIAP-1, Bcl-xL, Bcl-2, and  $\beta$ -actin. C. Prostate CSCs were grown in complete medium and treated with Rott (0, 0.5, 1 and 2  $\mu$ M) for 48 h. The Western blot analysis was performed to measure the expression of PI3K, Akt, p-Akt, mTOR, p-mTOR, and  $\beta$ -actin. D. AMPK shRNA inhibits Rott-induced autophagy. pEGFP-LC3-positive prostate CSCs were transfected with scrambled, AMPK shRNA and treated with Rott (2  $\mu$ M) for 24 h. Autophagy was measured as described in Fig. 3. Data represent mean  $\pm$  SD, \* $P$  < 0.05.

gradually increased (late apoptosis). Therefore, we report here both the percentage of early apoptosis (which indicates annexin-V-positive cells only) and the percentage cell death, which indicates the total number of annexin-V-FITC-plus propidium iodide staining cells and is representative of populations containing cells at both early and late stages of apoptosis.

Further, to confirm the role of Baf, 3-MA or CHX in apoptosis, we exposed the cells to Baf, 3-MA or CHX before treating with Rott. Treatment of prostate CSCs with Baf, 3-MA or CHX had no significant effect on apoptosis as assessed by flow cytometer using propidium iodide (PI) (Fig. 6A–D) and annexin-V/propidium iodide (Fig. 7A–E) through flow cytometry. Co-treatment of prostate CSCs with Baf, 3-MA or CHX inhibited Rott-induced apoptosis.

### 3.8. Inhibition of Atg7, or Beclin-1 by shRNA suppressed rottlerin-induced autophagy in prostate CSCs

We have recently demonstrated the requirement of Atg7 or Beclin-1 in Rott-induced autophagy. To investigate the mechanism of

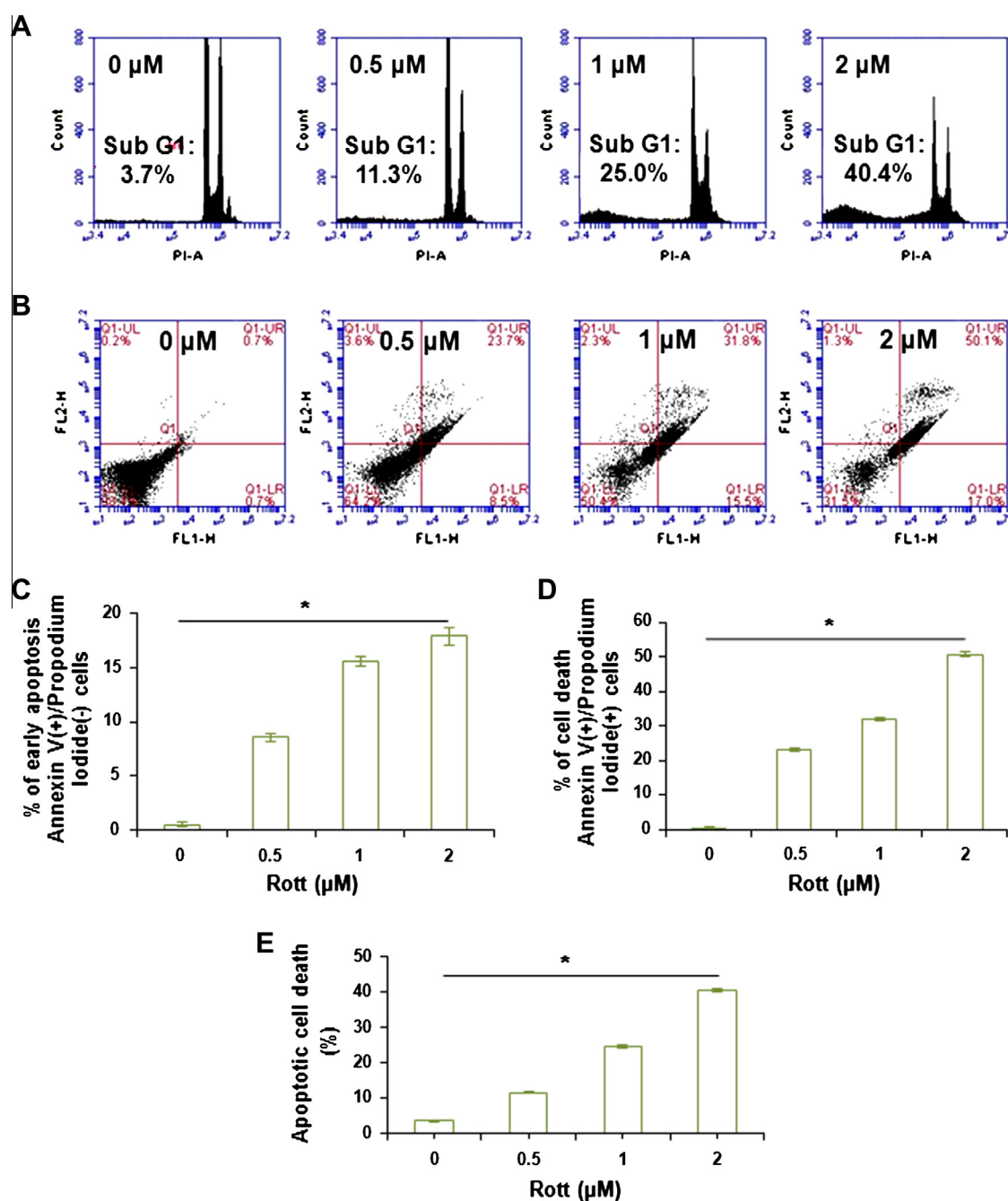


**Fig. 5.** Apoptosis induced by Rott in prostate CSCs. A. Cells were treated with Rott (0, 0.5, 1, and 2 μM) in complete medium for 48 h and apoptosis was measured by PI staining followed by flow cytometry. Data are the means of triplicate experiments. B. Time-course evaluation of spontaneous apoptosis of prostate CSCs treated with Rott (0, 0.5, 1 and 2 μM) in complete medium for 48 h and apoptosis was measured by annexin-V/PI staining followed by flow cytometry. Data are the means of triplicate experiments. Representative histograms are shown of Rott-treated prostate CSCs stained with annexin-V and propidium iodide. After 48 h of culture, three populations of cells were observed: viable cells (negatively stained, lower left quadrants), early apoptotic cells (annexin-V positive and propidium iodide negative, lower right quadrant) and cells in the late stages of apoptosis (annexin-V and propidium iodide positive, upper right quadrants). By increasing Rott concentration at 48 h, a greater number of prostate CSCs underwent the early and late stages of apoptosis. C. Kinetic measurement of cells undergoing the early stage of apoptosis in prostate CSCs. Cells staining with annexin-V only, showing the early stage of apoptosis (% of early apoptosis). D. Kinetic measurement of cells underwent the late stage of apoptosis in prostate CSCs. Cells staining with annexin-V alone and with both annexin-V and propidium iodide were combined, giving the total number of cells at both the early and late stages of apoptosis (% of cell death). E. Kinetic measurement of cells underwent apoptosis in prostate CSCs. Data are reported as the mean ± standard error (SE) of percentage of cells.  $N = 5$ ,  $^*P < 0.05$  when compared with Rott treated in an identical manner.

Rott-induced autophagy in prostate CSCs, we inhibited autophagy by Atg7 shRNA, or Beclin-1 shRNA. These plasmids have been previously validated in our laboratory [24]. As shown in (Fig. 7G), overexpression of Atg7 shRNA, or Beclin-1 shRNA suppressed Rott-induced autophagy, suggesting the requirement of these genes in Rott-induced autophagy.

#### 4. Discussion

The most outstanding features of the data presented above supported the induction of autophagy followed by apoptosis induced by plant derived chemopreventive drug Rott in prostate CSCs. In this study, we demonstrated that (1) Rott induces autophagy in

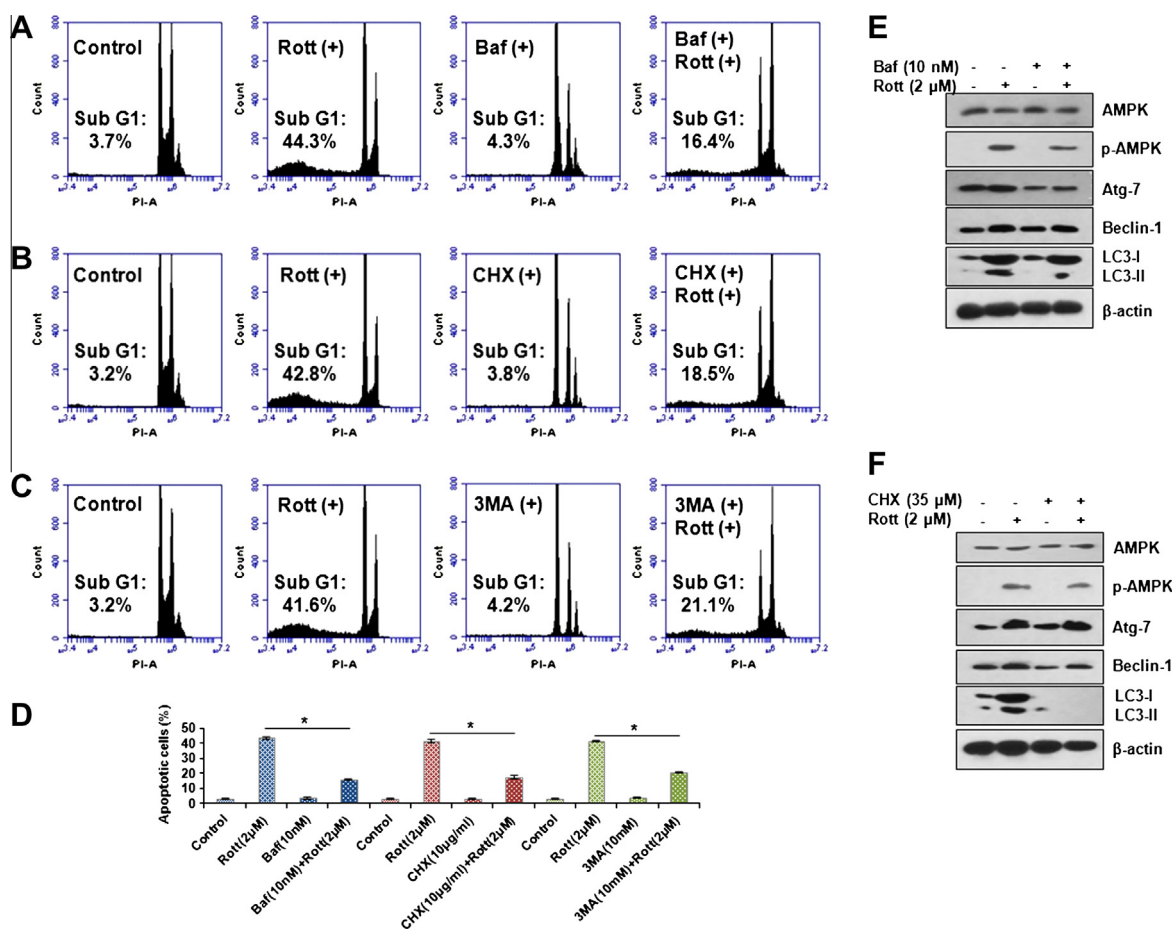


**Fig. 6.** Apoptosis induced by Rott in prostate CSCs measured by PI staining. Prostate CSCs were grown in complete medium and co-treated with Rott (2 μM) and Baf (10 nM), 3-MA (10 mM) or CHX (35 μM) for 48 h. A. Rott (2 μM) and Baf (10 nM). B. Rott (2 μM) and CHX (35 μM), and C. Rott (2 μM) and 3-MA (10 mM) in complete medium for 48 h. Apoptosis was measured by PI staining followed by flow cytometry. Data are the means of triplicate experiments. D. Kinetic measurement of cells underwent apoptosis in prostate CSCs. Data are reported as the mean ± standard error (SE) of percentage of cells.  $n = 5$ , \* $P < 0.05$  when compared with Rott (2 μM) treated in an identical manner. Prostate CSCs were grown in complete medium and co-treated with Rott (2 μM) and Baf (10 nM), 3-MA (10 mM) for 48 h, the cells were lysed and cellular proteins were then separated in SDS-polyacrylamide gels, after which they were transferred onto nitrocellulose membranes. The Western blot analysis was performed to measure the expression of AMPK, p-AMPK, conversion of LC3-I – LC3-II, Atg7, and Beclin-1. β-actin was used as a loading control, E. Prostate CSCs were pre-incubated with Baf (10 nM) for 2 h, followed by treatment with Rott (2 μM) in complete medium for 48 h, F. Prostate CSCs were pre-incubated with CHX (35 μM) for 2 h, followed by treatment with Rott (2 μM) in complete medium for 48 h.

prostate CSCs, (2) Rott induces apoptosis in prostate CSCs, (3) Rott induces autophagy in prostate CSCs by activating AMPK pathway, and (4) Rott induces apoptosis via inhibition of PI3K/Akt/mTOR pathway. These data demonstrated for the first time that Rott induces early autophagy by activating AMPK and apoptosis through PI3K/Akt/mTOR pathway in human prostate CSCs. One of the most interesting events in the early stage following treatment with Rott was the cytoplasmic vacuolation. These vacuoles were formed by Rott-induced autophagy and were identified by electron microscopy, acidic vesicular organelle staining, and transfection of green fluorescent protein-LC3. Remarkably, Rott-treated prostate CSCs did not undergo cell death at 24 h, while at late time points (48–72 h) showed significant cell death. Rott induced autophagy at 24 h, as evident by formation of autophagosomes and conversion of LC3-I – LC3-II form. These results indicate that treatment with Rott may induce autophagy at an early stage in prostate CSCs. Our study for the first time demonstrates that Rott treatment induces autophagy in prostate CSCs by activating AMPK pathway. Autophagy is a catabolic process during which damaged organelles and proteins are engulfed and degraded to provide metabolic needs. Autophagy is activated in response to various kinds of stress. Our results suggest that Rott induces autophagy in prostate

CSCs in a concentration dependent manner as analyzed by electron microscopy.

Rott-induced apoptosis was mediated through a decrease of mitochondrial membrane potential and translocation of AIF into nucleus at a late time point [36,37]. Moreover, the inhibition of Rott-induced autophagy with Baf, 3-MA or CHX slows down apoptosis (Fig. 7). On the other hand, Rott treatment in the presence of Baf, 3-MA or CHX lead to decreased expression of LC3 and Atg7 when compared to the cells treated either with Rott or with inhibitors alone, suggesting increased autophagic potentials. All three Baf, 3-MA or CHX inhibit the fusion between autophagosomes as well as autolysosomes, thus prevent the execution step of autophagy [38]. However, our results from flow cytometry demonstrated that Baf, 3-MA or CHX inhibits Rott-induced apoptosis in prostate CSCs.

In this study, Rott was found to induce autophagy in prostate CSCs, including formation of autophagosomes, redistribution of LC3 and induction of autophagy related proteins including Atg5, Atg7, Atg12 and Beclin-1 at 24 h. The antiapoptotic protein, Bcl-2, inhibits the Beclin-1 dependent autophagy [39,40]. Rott significantly inhibited Bcl-2 and Bcl-xL expression, and induced Atg5, Atg7, Atg12 and Beclin-1. Moreover, Baf, 3-MA or CHX inhibited

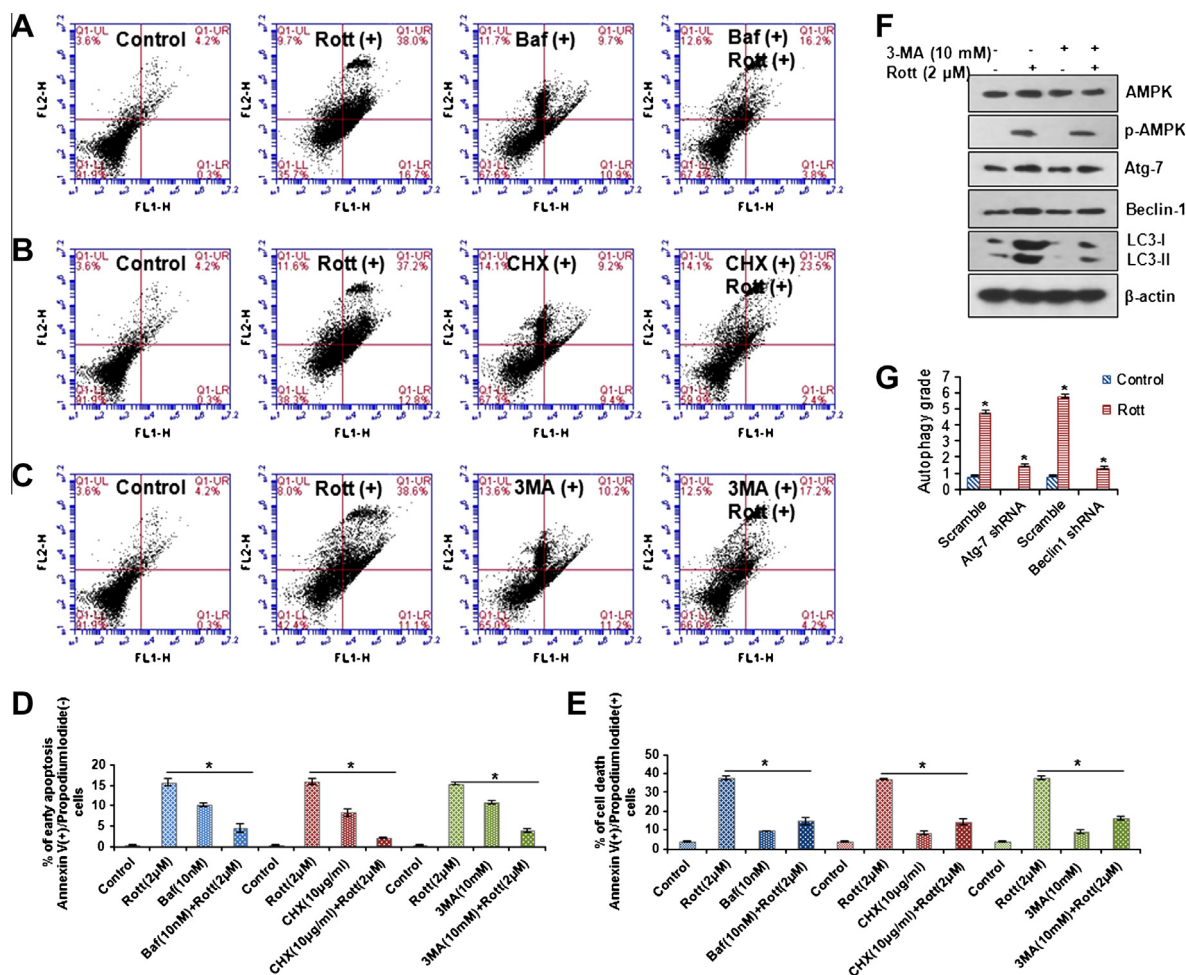


**Fig. 7.** Apoptosis induced by Rott in prostate CSCs measured by annexin-V/PI staining. The time-course evaluation of spontaneous apoptosis of prostate CSCs treated with Rott (0, 0.5, 1, and 2  $\mu$ M) in complete medium for 48 h and apoptosis was measured by annexin-V/PI staining followed by flow cytometry. Data are the means of triplicate experiments. Representative histograms are shown of Rott-treated prostate CSCs stained with annexin-V and propidium iodide. After 48 h of culture, three populations of cells were observed: viable cells (negatively stained, lower left quadrant), early apoptotic cells (annexin-V positive and propidium iodide negative, lower right quadrant) and cells in the late stages of apoptosis (annexin-V and propidium iodide positive, upper right quadrant). By increasing Rott concentration at 48 h, a greater number of prostate CSCs underwent the early and late stages of apoptosis. Prostate CSCs were grown in complete medium and co-treated with Rott (2  $\mu$ M) and Baf (10 nM), 3-MA (10 mM) or CHX (35  $\mu$ M) for 48 h. A. Rott (2  $\mu$ M) and Baf (10 nM). B. Rott (2  $\mu$ M) and CHX (35  $\mu$ M), and C. Rott (2  $\mu$ M) and 3-MA (10 mM) in complete medium for 48 h. D. Kinetic measurement of cells underwent early apoptosis in prostate CSCs. E. Kinetic measurement of cells underwent late apoptosis in prostate CSCs. Data are reported as the mean  $\pm$  standard error (SE) of percentage of cells.  $n = 5$ ,  $^*P < 0.05$  when compared with Rott (2  $\mu$ M) treated in an identical manner. Prostate CSCs were grown in complete medium and co-treated with Rott (2  $\mu$ M) and Baf (10 nM) and 3-MA (10 mM) for 48 h, the cells were lysed and cellular proteins were then separated in SDS-polyacrylamide gels, after which they were transferred onto nitrocellulose membranes. The Western blot analysis was performed to measure the expression of AMPK, p-AMPK, conversion of LC3-I – LC3-II, Atg7 and Beclin-1,  $\beta$ -actin was used as a loading control, F. Prostate CSCs were pre-incubated with 3-MA (10 mM) for 2 h, followed by treatment with Rott (2  $\mu$ M) in complete medium for 48 h. G. Knockdown of Atg7 and Beclin-1 inhibited autophagy. Scrambled shRNA, sh-Atg7 and sh-Beclin-1 pancreatic CSCs were seeded on fibronectin-coated coverslips and treated with Rott (0, 0.5, 1 and 2  $\mu$ M) for 24 h. Cells were visualized under a fluorescence microscope to examine the expression of LC3-II. LC3 punctate dot increases by increasing Rott concentration in scramble prostate CSCs. LC3 punctate dot did not appear in case of knockdown Atg7 and Beclin-1. Data are reported as the mean  $\pm$  standard error (SE) of percentage of cells.  $n = 5$ ,  $^*P < 0.05$  when compared with Rott (2  $\mu$ M) treated in an identical manner. Atg-7, or Beclin-1 shRNA inhibits Rott-induced autophagy. pEGFP-LC3-positive prostate CSCs were transfected with scrambled, Atg-7 shRNA, or Beclin-1 shRNA treated with Rott (2  $\mu$ M) for 24 h. Autophagy was measured as described in Fig. 3. Data represent mean  $\pm$  SD,  $^*P < 0.05$ . (For interpretation of the references to colour in this figure legend, the reader is referred to the web version of this article.)

Rott induced conversion of LC3-I – LC3-II, and expression of autophagy-related proteins Atg5, Atg7, Atg12 and Beclin-1 at 24 h (see Fig. 8).

We have also studied the autophagic activity of prostate CSCs by knocking down Atg7 and Beclin-1 in prostate CSCs. We have observed that prostate CSCs did not form autophagic vacuoles by knocking down Atg7 and Beclin-1. Atg7 and Beclin-1 knocked down prostate CSCs were unable to induce autophagy even after treatment with Rott. These results strongly suggest that Atg7 and Beclin-1 plays an important role in the formation of autophagosomes and Rott-induced autophagy in prostate CSCs. Our previous studies on pancreatic CSCs also suggest that the Rott cannot restore

the autophagic properties after knocking down Atg7 and Beclin-1 [24].

Our study demonstrates that co-treatment of the CSCs with Rott and Baf, 3-MA or CHX inhibited the Rott induced autophagy and slows down the apoptosis. Therefore, Rott-induced autophagy may play some role in apoptosis. Apoptosis is an important tumor suppressor mechanism that is blocked in the majority of human cancers, due to the over activation of the AMPK and PI3K/Akt/mTOR pathway [32]. Activation of AMPK and PI3K/Akt/mTOR pathway regulates transcription factors that modulate distinct sets of genes involved in cell cycle, apoptosis, oxidative stress and DNA repair [32]. Treatment of prostate CSCs with Rott increased the levels

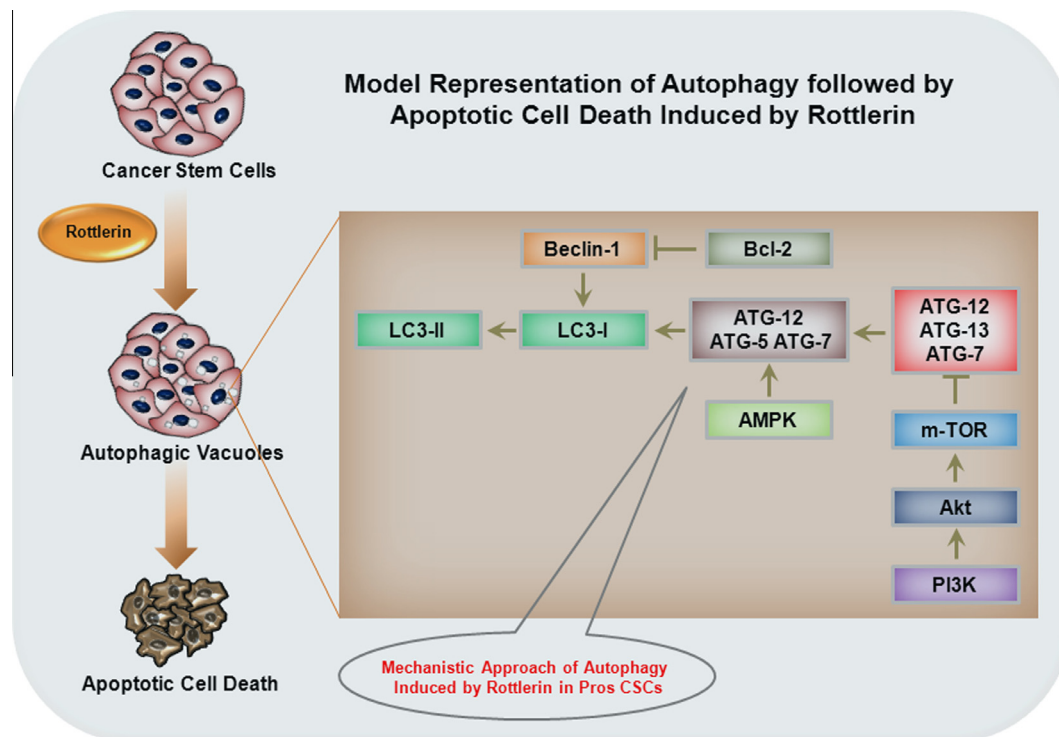


**Fig. 8.** Model summarizing the autophagy and apoptosis in prostate CSCs induced by plant derived chemopreventive agent Rott. Rott enhances autophagy in prostate CSCs that leads to the apoptosis via cytoplasmic vacuolation and autophagosomes formation. Insert shows the deactivation of Bcl-2, PI3K, p-Akt and p-mTOR pathway that activates autophagosomes formation and autophagy in prostate CSCs, and activation of p-AMPK by Rott. To get the stable autophagosomes, LC3 undergoes post-translational processing and LC3-I is converted to LC3-II.

of phosphorylated AMPK. Furthermore, downregulation of constitutively active PI3K/Akt/mTOR and upregulation of AMPK rendered prostate CSCs sensitive to Rott. Rott induced significant apoptosis in prostate CSCs at 48–72 h by inhibiting phosphorylation of Akt and mTOR, and expression of Bcl-2, Bcl-xL, cIAP1 and XIAP, up-regulation of AMPK and Bax, and activation of caspase-3 and -9. Therefore, we understood that the Rott-induced apoptosis is also dependent on the AMPK and PI3K/Akt/mTOR pathway. These observations suggest that Rott can induce autophagy leading to apoptosis in prostate CSCs. Our results indicate that Rott causes early autophagy and late apoptosis through inhibition of PI3K/Akt/mTOR pathway in human prostate CSCs.

In summary, the potential effect of Rott in induction of early stage autophagy via activation of AMPK pathway and apoptosis via inhibiting PI3K/Akt/mTOR pathway in human prostate CSCs provided potential mechanism of autophagy and apoptosis induced by Rott in prostate CSCs. A better understanding of the biology of autophagy will help us in developing autophagy-based therapeutic interventions for prostate cancer.

#### 4.1. Statistical analysis

Experiments were conducted thrice independently in triplicate. Data are shown as means  $\pm$  S.D. (standard deviation) or S.E. (standard error) of values obtained from the experiments. Significant differences were evaluated using the student's *t*-test.

#### Conflict of interest

All the authors of this paper have declared “no conflict of interest”.

#### Acknowledgment

We thank our lab members for critical reading of the manuscript.

#### References

- [1] J.J. Lum, D.E. Bauer, M. Kong, M.H. Harris, C. Li, T. Lindsten, C.B. Thompson, Growth factor regulation of autophagy and cell survival in the absence of apoptosis, *Cell* 120 (2005) 237–248.
- [2] J. Onodera, Y. Ohsumi, Autophagy is required for maintenance of amino acid levels and protein synthesis under nitrogen starvation, *J. Biol. Chem.* 280 (2005) 31582–31586.
- [3] Z.Y. Yue, S.K. Jin, C.W. Yang, A.J. Levine, N. Heintz, Beclin 1, an autophagy gene essential for early embryonic development, is a haploinsufficient tumor suppressor, *P. Natl. Acad. Sci. USA* 100 (2003) 15077–15082.
- [4] V. Deretic, M. Delgado, I. Vergne, S. Master, S. De Haro, M. Ponpuak, S. Singh, Autophagy in immunity against mycobacterium tuberculosis: a model system to dissect immunological roles of autophagy, *Curr. Top Microbiol.* 335 (2009) 169–188.
- [5] D.J. Klionsky, S.D. Emr, Cell biology – autophagy as a regulated pathway of cellular degradation, *Science* 290 (2000) 1717–1721.
- [6] M.C. Maiuri, E. Zalckvar, A. Kimchi, G. Kroemer, Self-eating and self-killing: crosstalk between autophagy and apoptosis, *Nat. Rev. Mol. Cell Bio.* 8 (2007) 741–752.
- [7] Z. Talloczy, W.X. Jiang, H.W. Virgin, D.A. Leib, D. Scheuner, R.J. Kaufman, E.L. Eskelinen, B. Levine, Regulation of starvation- and virus-induced autophagy by the eIF2 alpha kinase signaling pathway, *P. Natl. Acad. Sci. USA* 99 (2002) 190–195.
- [8] T. Kanzawa, I.M. Germano, T. Komata, H. Ito, Y. Kondo, S. Kondo, Role of autophagy in temozolomide-induced cytotoxicity for malignant glioma cells, *Cell Death Diff.* 11 (2004) 448–457.
- [9] T. Kanzawa, Y. Kondo, H. Ito, S. Kondo, I. Germano, Induction of autophagic cell death in malignant glioma cells by arsenic trioxide, *Cancer Res.* 63 (2003) 2103–2108.
- [10] S. Paglin, T. Hollister, T. Delohery, N. Hackett, M. McMahon, E. Sphicas, D. Domingo, J. Yahalom, A novel response of cancer cells to radiation involves autophagy and formation of acidic vesicles, *Cancer Res.* 61 (2001) 439–444.
- [11] E.H. Baehrecke, Autophagy: dual roles in life and death?, *Nat. Rev. Mol. Cell Biol.* 6 (2005) 505–510.

- [12] G. Kroemer, G. Marino, B. Levine, Autophagy and the integrated stress response, *Mol. Cell* 40 (2010) 280–293.
- [13] C.Y. Xu, B. Bailly-Maitre, J.C. Reed, Endoplasmic reticulum stress: cell life and death decisions, *J. Clin. Invest.* 115 (2005) 2656–2664.
- [14] M. Hoyer-Hansen, M. Jaattela, Connecting endoplasmic reticulum stress to autophagy by unfolded protein response and calcium, *Cell Death Diff.* 14 (2007) 1576–1582.
- [15] B. Levine, J. Yuan, Autophagy in cell death: an innocent convict?, *J. Clin. Invest.* 115 (2005) 2679–2688.
- [16] J.F. Geng, M. Baba, U. Nair, D.J. Klionsky, Quantitative analysis of autophagy-related protein stoichiometry by fluorescence microscopy (vol. 182, p. 129, *J. Cell Biol.* 183 (2008) (2008) 1175).
- [17] D. Gozuacik, A. Kimchi, Autophagy as a cell death and tumor suppressor mechanism, *Oncogene* 23 (2004) 2891–2906.
- [18] T. Nemoto, I. Tanida, E. Tanida-Miyake, N. Minematsu-Ikeguchi, M. Yokota, M. Ohsumi, T. Ueno, E. Kominami, The mouse Apg10 homologue, an E2-like enzyme for Apg12p conjugation, facilitates MAP-LC3 modification, *J. Biol. Chem.* 278 (2003) 39517–39526.
- [19] N. Mizushima, A. Yamamoto, M. Hatano, Y. Kobayashi, Y. Kabeya, K. Suzuki, T. Tokuhisa, Y. Ohsumi, T. Yoshimori, Dissection of autophagosome formation using Apg5-deficient mouse embryonic stem cells, *J. Cell Biol.* 152 (2001) 657–667.
- [20] N. Kourtis, N. Tavernarakis, Autophagy and cell death in model organisms, *Cell Death Diff.* 16 (2009) 21–30.
- [21] X.P. Qu, J. Yu, G. Bhagat, N. Furuya, H. Hibshoosh, A. Troxel, J. Rosen, E.L. Eskelinen, N. Mizushima, Y. Ohsumi, G. Cattoretti, B. Levine, Promotion of tumorigenesis by heterozygous disruption of the beclin 1 autophagy gene, *J. Clin. Invest.* 112 (2003) 1809–1820.
- [22] E.V. Batrakova, H.E. Gendelman, A.V. Kabanov, Cell-mediated drug delivery, *Expert Opin. Drug Del.* 8 (2011) 415–433.
- [23] A.M. Martelli, C. Evangelisti, M.Y. Follo, G. Ramazzotti, M. Fini, R. Giardino, L. Manzoli, J.A. McCubrey, L. Cocco, Targeting the phosphatidylinositol 3-kinase/Akt/mammalian target of rapamycin signaling network in cancer stem cells, *Curr. Med. Chem.* 18 (2011) 2715–2726.
- [24] B.N. Singh, D. Kumar, S. Shankar, R.K. Srivastava, Rottlerin induces autophagy which leads to apoptotic cell death through inhibition of PI3K/Akt/mTOR pathway in human pancreatic cancer stem cells, *Biochem. Pharmacol.* 84 (2012) 1154–1163.
- [25] Y. Shao, Z. Gao, P.A. Marks, X. Jiang, Apoptotic and autophagic cell death induced by histone deacetylase inhibitors, *Proc. Natl. Acad. Sci. USA* 101 (2004) 18030–18035.
- [26] R.A. Gonzalez-Polo, M. Niso-Santano, M.A. Ortiz-Ortiz, A. Gomez-Martin, J.M. Moran, L. Garcia-Rubio, J. Francisco-Morcillo, C. Zaragoza, G. Soler, J.M. Fuentes, Inhibition of paraquat-induced autophagy accelerates the apoptotic cell death in neuroblastoma SH-SY5Y cells, *Toxicol. Sci.* 97 (2007) 448–458.
- [27] A. Herman-Antosiewicz, D.E. Johnson, S.V. Singh, Sulforaphane causes autophagy to inhibit release of cytochrome C and apoptosis in human prostate cancer cells, *Cancer Res.* 66 (2006) 5828–5835.
- [28] T.M. Nguyen, I.V. Subramanian, A. Kelekar, S. Ramakrishnan, Kringle 5 of human plasminogen, an angiogenesis inhibitor, induces both autophagy and apoptotic death in endothelial cells, *Blood* 109 (2007) 4793–4802.
- [29] S. Luo, D.C. Rubinsztein, Atg5 and Bcl-2 provide novel insights into the interplay between apoptosis and autophagy, *Cell Death Diff.* 14 (2007) 1247–1250.
- [30] P.K. Kandala, S.K. Srivastava, Regulation of macroautophagy in ovarian cancer cells in vitro and in vivo by controlling glucose regulatory protein 78 and AMPK, *Oncotarget* 3 (2012) 435–449.
- [31] M. Gschwendt, H.J. Muller, K. Kielbassa, R. Zang, W. Kittstein, G. Rincke, F. Marks, Rottlerin, a novel protein-kinase inhibitor, *Biochem. Biophys. Res. Commun.* 199 (1994) 93–98.
- [32] S. Saiiki, Y. Sasazawa, Y. Imamichi, S. Kawajiri, T. Fujimaki, I. Tanida, H. Kobayashi, F. Sato, S. Sato, K.I. Ishikawa, M. Imoto, N. Hattori, Caffeine induces apoptosis by enhancement of autophagy via PI3K/Akt/mTOR/p70S6K inhibition, *Autophagy* 7 (2011) 176–187.
- [33] S. Shankar, D. Nall, S.N. Tang, D. Meeker, J. Passarini, J. Sharma, R.K. Srivastava, Resveratrol inhibits pancreatic cancer stem cell characteristics in human and kras(G12D) transgenic mice by inhibiting pluripotency maintaining factors and epithelial–mesenchymal transition, *PLoS ONE* 6 (2011).
- [34] R. Nanta, D. Kumar, D. Meeker, M. Rodova, P.J. Van Veldhuizen, S. Shankar, R.K. Srivastava, NVP-LDE-225 (Erismodegib) inhibits epithelial–mesenchymal transition and human prostate cancer stem cell growth in NOD/SCID IL2Rgamma null mice by regulating Bmi-1 and microRNA-128, *Oncogenesis* 2 (2013) e42.
- [35] A. Yamamoto, Y. Tagawa, T. Yoshimori, Y. Moriyama, R. Masaki, Y. Tashiro, Bafilomycin A1 prevents maturation of autophagic vacuoles by inhibiting fusion between autophagosomes and lysosomes in rat hepatoma cell line, H-4-II-E cells, *Cell Struct. Funct.* 23 (1998) 33–42.
- [36] S.A. Susin, H.K. Lorenzo, N. Zamzami, I. Marzo, B.E. Snow, G.M. Brothers, J. Mangion, E. Jacotot, P. Costantini, M. Loeffler, N. Larochette, D.R. Goodlett, R. Aebbersold, D.P. Siderovski, J.M. Penninger, G. Kroemer, Molecular characterization of mitochondrial apoptosis-inducing factor, *Nature* 397 (1999) 441–446.
- [37] Y. Wang, V.L. Dawson, T.M. Dawson, Poly(ADP-ribose) signals to mitochondrial AIF: a key event in parthanatos, *Exp. Neurol.* 218 (2009) 193–202.
- [38] Y.-p. Yang, L.-f. Hu, H.-f. Zheng, C.-j. Mao, W.-d. Hu, K.-p. Xiong, F. Wang, C.-f. Liu, Application and interpretation of current autophagy inhibitors and activators, *Acta Pharmacol. Sin.* 34 (2013) 625–635.
- [39] M. Gaytán, C. Morales, J.E. Sánchez-Criado, F. Gaytán, Immunolocalization of beclin 1, a bcl-2-binding, autophagy-related protein, in the human ovary: possible relation to life span of corpus luteum, *Cell Tissue Res.* 331 (2) (2008) 509–517.
- [40] H. Hu, Y. Chai, L. Wang, J. Zhang, H.J. Lee, S.H. Kim, J. Lu, Pentagalloylglucose induces autophagy and caspase-independent programmed deaths in human PC-3 and mouse TRAMP-C2 prostate cancer cells, *Mol. Cancer Ther.* 8 (2009) 2833–2843.